Progress In Electromagnetics Research C, Vol. 130, 107–116, 2023

Anti-Reflection Coating on Solar Cell

Samar Bahadur Chauhan* and Sudesh Kumar Singh

Abstract—To utilise maximum amount of available optical energy it is necessary to design a solar cell with minimum reflectance from its surface. Broadband anti-reflection coatings are essential elements for improving the photo current generation of photovoltaic modules. The vast majority of antireflection coatings are required for matching an optical element into air. In this work, we choose the substrate of the structure that has an index sufficiently higher than the available thin film materials to enable the design of high performance antireflection coatings. This high index substrate is silicon (Si) of refractive index 3.54 at design wavelength 500 nm. Quarter wavelength optical thicknesses (QWOTs) of films of various dielectrics are coated with refractive indices calculated by "Root-Principle". The reflection spectra of visible radiation in normal and oblique incidence with antireflection coatings up to six layers will be analysed to achieve nearly zero reflectance.

1. INTRODUCTION

Solar cell is a device to convert solar energy into electrical energy. About $1\,\mathrm{kW/m^2}$ is available from Sun in particular sunny locations. Only one fourth of this power is converted into electrical power. A Si solar cell transmits only 30% of incident radiation energy, and it reflects remaining part back. Of all the possible applications, antireflection coatings (ARC) [1, 2] have had the greatest impact on optoelectronics. In general, the reflection occurs on the surfaces between two media with different refractive indices. However, the reflection can be reduced by thin ARC. The concept of ARC was introduced for the first time by Lord Rayleigh. Researchers have already used several thin film layers with different refractive index (RI) values for ARC. Yu et al. [3] in 2013 and again in 2015 [4] demonstrated the performance of semi-transparent polymer solar cells and calculated, practically, efficiency and power conversion efficiency. Geetha Priyadarshini and Sharma in 2015 [5] designed single, double, and triple layers as coatings using SiO_2, TiO_2, and ZnO on a glass substrate of terrestrial solar panel to get broadband antireflection property. Matsuoka et al., in 2018 [6] studied in optical range 7–12 μm and 10–12 μm ranges for ARC of YF_3, ZnS, and Ge on substrate InP to get reflection below 1%. Ismail Fathima and Joseph Wilson, in 2019 [7], studied $MgF_2/ZnSe/ZrO_2$ ARC in ZnO dye-sensitized solar cell (DSSC) and found that the performance of DSSC was largely dependent on the ZnO film thickness. Deka and Mohammed in 2020 [8] used gold and silver nanoparticles in between MgF_2 and polymethyl methacrylate as ARC design for selective peak absorption on desired range of near UV region. Guo et al., in 2021 [9], designed ARC of high index material Ta_2O_5 and low index material SiO_2 on substrate supphire glass. Using up to 22 layers ARC, the reflectance was only 1.5% for optical range 400–2000 nm, while the 36 layers ARC provided 0.8% of reflectance, coated on both sides of substrate.

The ARC plays a vital role in antiglare displays [10], automobile dashboards [11], solar cells [12–15], and other optical systems. To increase efficiency of photovoltaic (PV) cell, there should be multilayer ARC. By precisely controlling the refractive index (RI) values of chosen film material, the thickness of

Received 16 December 2022, Accepted 10 February 2023, Scheduled 22 February 2023
* Corresponding author: Samar Bahadur Chauhan (samariet2@gmail.com).
The authors are with the Department of Physics, T. D. P. G. College, Jaunpur (U.P.) 222002, India.

each film and also selecting four or five layers of deposition on the substrate, the surface reflection can be reduced to nearly zero.

In this proposed work, we take quarter wavelength layer thickness for ARC [16]. Taking substrate Si of RI $n_s = 3.54$ at wavelength $(\lambda) = 500\,\text{nm}$, other dielectric materials are selected depending on the RI obtained by calculation based on 'Root-Principle' [17] to get nearly zero reflectance. The theory of design, reflectance spectrum analysis, results and discussion, and finally conclusion will be given in coming sections.

2. THEORY

2.1.

The optical parameters transmittance and reflectance for multilayer optical coatings [18] are calculated using transfer matrix method (TMM) [19]. We define optical admittance $Y = C/B$, where B and C are normalised electric and magnetic fields related to

$$\begin{bmatrix} B \\ C \end{bmatrix} = \prod_{i=1}^{N} \begin{bmatrix} \cos\phi_i & j\sin\phi_i/\eta_i \\ j\eta_i\sin\phi_i & \cos\phi_i \end{bmatrix} \begin{bmatrix} 1 \\ \eta_s \end{bmatrix} \tag{1}$$

We have taken phase difference ϕ_i for two successive reflected waves in the ith layer given by

$$\phi_i = \frac{2\pi}{\lambda} n_i d_i \cos\theta_i \tag{2}$$

where n_i is the RI, d_i the thickness, and θ_i the angle of incidence for the ith layer. For the assembly of N layers, the characteristic matrix is given by

$$\begin{pmatrix} B \\ C \end{pmatrix} = [M_1]\,[M_2]\,[M_3]\_\_\_\_\_\_\_\,[M_N] \begin{bmatrix} 1 \\ \eta_s \end{bmatrix} \tag{3}$$

where,

$$M_i = \begin{bmatrix} \cos\phi_i & j\sin\phi_i/\eta_i \\ j\eta_i\sin\phi_i & \cos\phi_i \end{bmatrix} \tag{4}$$

and M_i is the 2×2 matrix associated with the ith layer.

For s-polarisation or in TE mode, the characteristic admittance is given by

$$\eta_i = \eta_0 n_i \cos\theta_i \tag{5}$$

and for p-polarisation or in TM mode

$$\eta_i = \frac{\eta_0 n_i}{\cos\theta_i} \tag{6}$$

where η_0 is the admittance of free space.

From above equations, the reflectance can be given by

$$R = \left|\frac{\eta_0 - Y}{\eta_0 + Y}\right|^2 \tag{7}$$

and hence the transmittance will be given by

$$T = 1 - R \tag{8}$$

2.2.

For antireflection from the surface of PV cell, we take quarter wavelength optical thickness (QWOT) of each film. We employ 'Root-Principle' [10] to calculate RI n_{ij} of each film material using

$$n_{i(j=1)} = \sqrt{n_s n_{(i-1)(j=1)}}, \quad \textit{for the } \text{first layer on substrate} \tag{9}$$

$$n_{ij} = \sqrt{n_{(i-1)(j-1)}\, n_{(i-1)j}} \tag{10}$$

$$n_{i(j=i)} = \sqrt{n_{(i-1)(j=i-1)}\, n_0}, \quad \textit{for the } \text{last layer on substrate} \tag{11}$$

3. RESULTS AND DISCUSSION

In our case, $n_{00} = n_{10} = n_s = 3.54$ for substrate and $n_{01} = n_0 = 1$ for air.

Using Equations (9), (10), and (11), the value of n_{ij} can be calculated, e.g.,

$$n_{11} = (n_s\, n_0)^{1/2} = 1.8815$$
$$n_{21} = (n_s^3\, n_0)^{1/4} = 2.5808$$
$$n_{22} = (n_s\, n_0^3)^{1/4} = 1.3717 \text{ and so on.}$$

These calculated values of RI for different coating materials are given in Table 1.

Table 1. Calculated RI of coated materials with number of layers.

Number of coated Layers	RI of coatedmaterial
1	$n_{11} = 1.8815$
2	$n_{21} = 2.5808$ $n_{22} = 1.3717$
3	$n_{31} = 3.0226$ $n_{32} = 1.8815$ $n_{33} = 1.7712$
4	$n_{41} = 3.2711$ $n_{42} = 2.3847$ $n_{43} = 1.4844$ $n_{44} = 1.0822$
5	$n_{51} = 3.4029$ $n_{52} = 2.793$ $n_{53} = 1.8815$ $n_{54} = 1.2675$ $n_{55} = 1.0403$
6	$n_{61} = 3.4708$ $n_{62} = 3.0830$ $n_{63} = 2.2937$ $n_{64} = 1.5443$ $n_{65} = 1.4823$ $n_{66} = 1.0199$

Figure 1 shows the reflection spectra of Si without and with coatings at normal incidence. The blue curve shows up to 70% reflection at design wavelength $\lambda_0 = 500$ nm for Si without coating. On coating with layers $N = 1, 2, 3, 4, 5$, and 6, the bandwidths for reflectance $< 1\%$ are shown in spectral curves and also given in Table 2 at $\theta = 0°$. Thus as N increases, the bandwidth increases from 95.8 nm to maximum 701.9 nm.

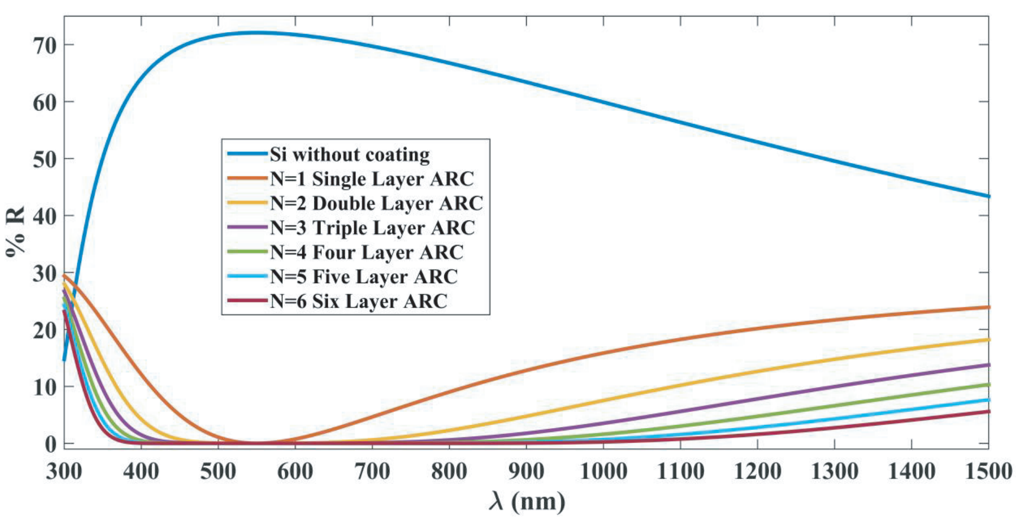

Figure 1. Reflection spectra of Si without coating and Si with ARC for $N = 1, 2, 3, 4, 5, 6$ layers at $\theta = 0°$.

Figures 2(a) to 2(f) show reflection spectra in oblique incidence in TE mode for $N = 1$ to $N = 6$ in each case.

The bandwidth for reflectance $< 1\%$ increases in each case with the increase in N, but it decreases with the increase of angle of incidence from $0°$ to $75°$. From these spectral curves, the calculated values of bandwidths are given in Table 2. Thus the best result for nearly zero reflectance is obtained at $\theta = 0°$ and $N = 6$, for high quality ARC.

Figures 3(a) to 3(f) also show reflection spectra in oblique incidence but in TM mode for $N = 1$ to $N = 6$, respectively.

Similar to that in TE mode, here in TM mode also, for the reflectance $< 1\%$, the bandwidth

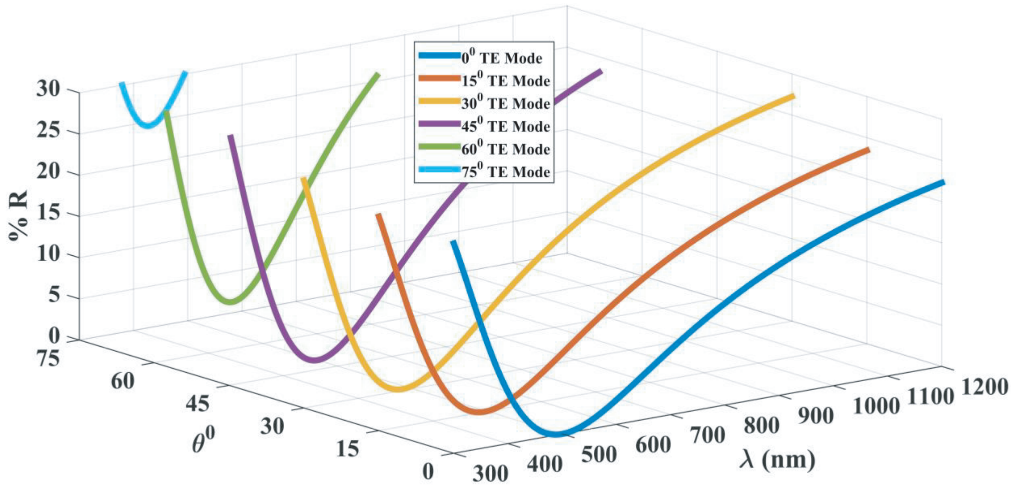

(a)

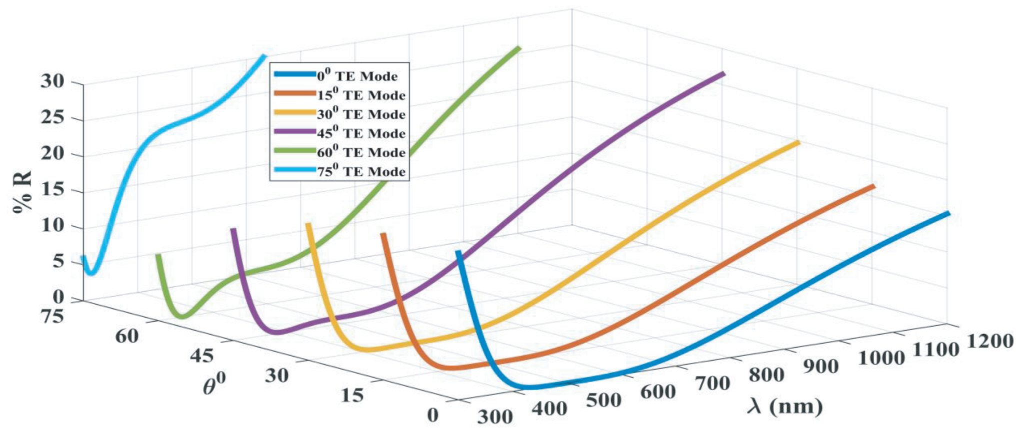

(b)

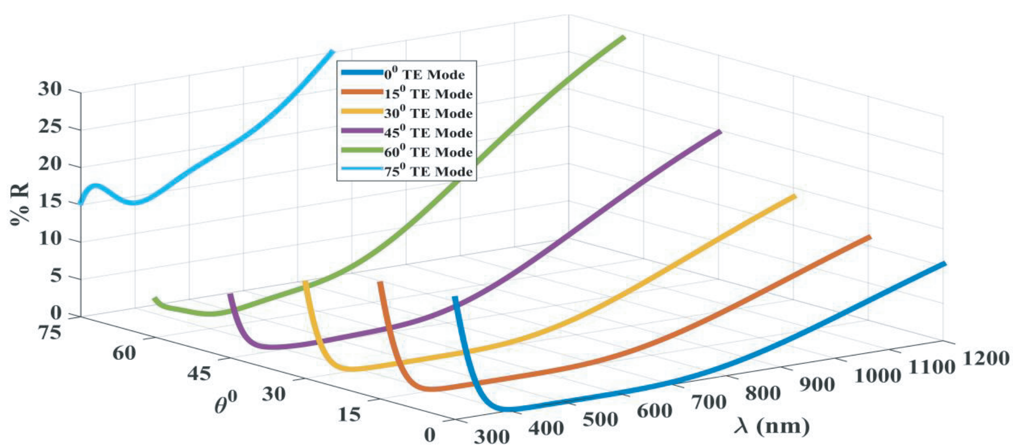

(c)

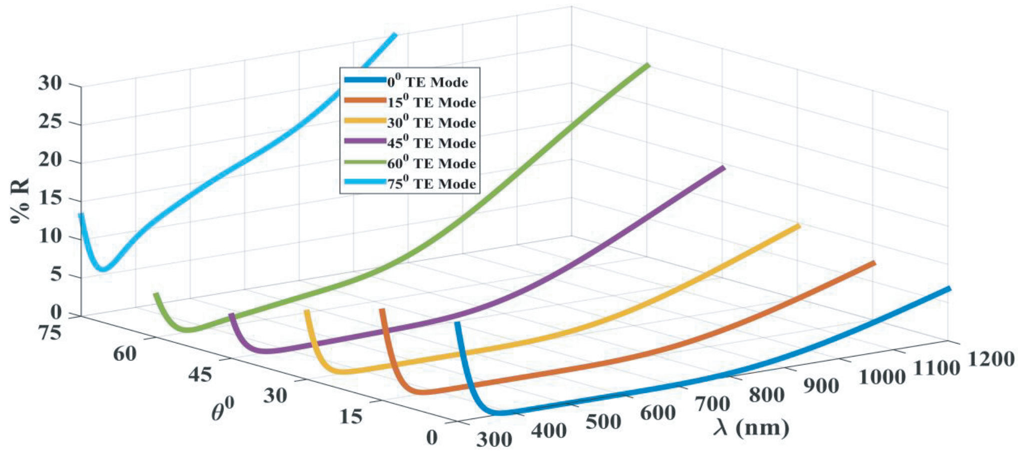

(d)

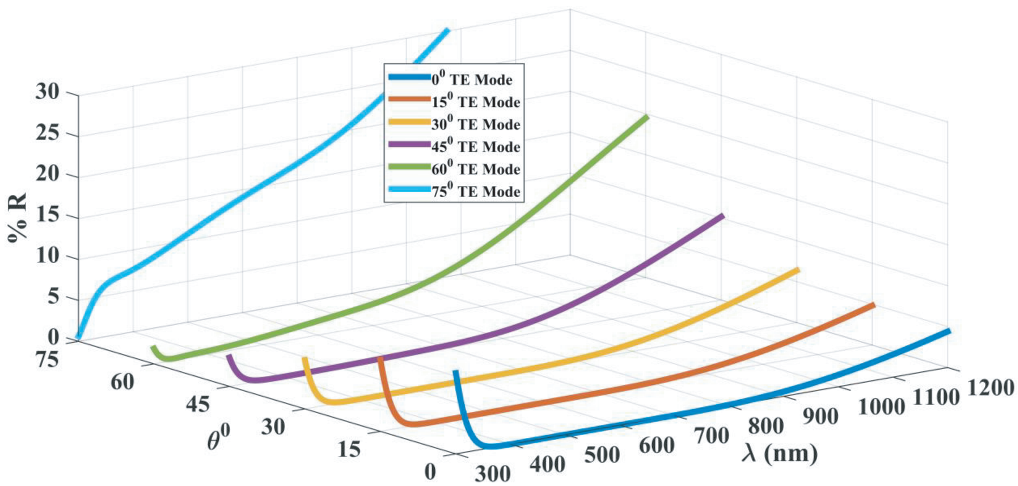

(e)

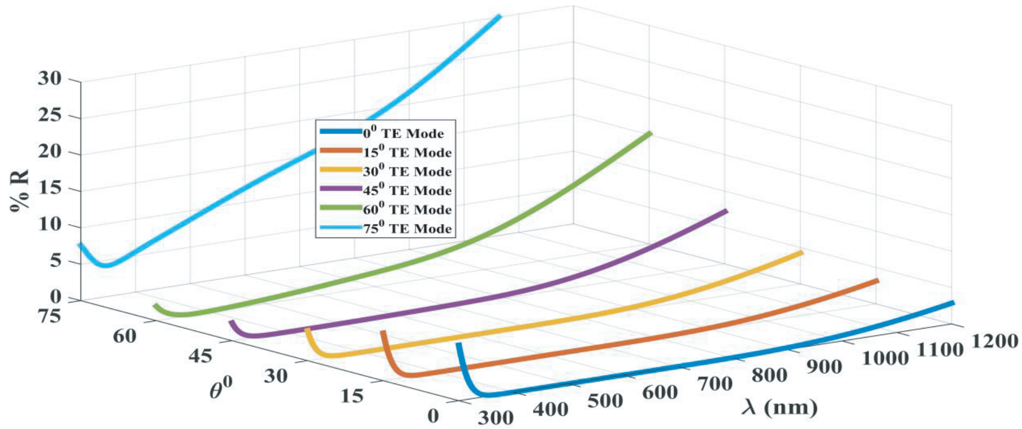

(f)

Figure 2. (a) Refection spectra of single coated materials in oblique incidence in TE mode. (b) Refection spectra of double coated materials in oblique incidence in TE mode. (c) Refection spectra of triple coated materials in oblique incidence in TE mode. (d) Refection spectra of four fold coated materials in oblique incidence in TE mode. (e) Refection spectra of five fold coated materials in oblique incidence in TE mode. (f) Refection spectra of six fold coated materials in oblique incidence in TE mode.

Table 2. Bandwidth for reflectance < 1% in oblique incidence for number of coated layers in TE mode.

Number of Coated layer	Band width $\Delta\lambda$ (nm) for reflectance < 1% in TE mode at angle of incidence					
	0°	**15°**	**30°**	**45°**	**60°**	**75°**
1	456.6 ∼ 552.4 = 95.8	447.5 ∼ 522.5 = 91.7	447.5 ∼ 522.5 = 75	-	-	-
2	399.5 ∼ 668.1 = 268.6	395 ∼ 659.9 = 264.9	381.5 ∼ 629.5 = 248	358 ∼ 532.6 = 174.6	327.9 ∼ 370.2 = 42.3	-
3	369.4 ∼ 772.4 = 403	367.1 ∼ 762.6 = 395.5	357.8 ∼ 731 = 373.2	352.7 ∼ 650 = 297.3		-
4	351.3 ∼ 867.9 = 516.6	349 ∼ 856.3 = 507.3	340.5 ∼ 821.8 = 481.3	335.3 ∼ 736.7 = 401.4	335.5 ∼ 445.3 = 109.8	-
5	338.8 ∼ 954.1 = 615.3	335.9 ∼ 942 = 606.1	328.4 ∼ 903.6 = 575.2	321.1 ∼ 814.8 = 493.7	308.1 ∼ 507.7 = 199.6	-
6	331.1 ∼ 1033 = 701.9	327 ∼ 1020 = 693	320.4 ∼ 977.8 = 657.4	314 ∼ 885.3 = 571.3	315.6 ∼ 568 = 252.4	-

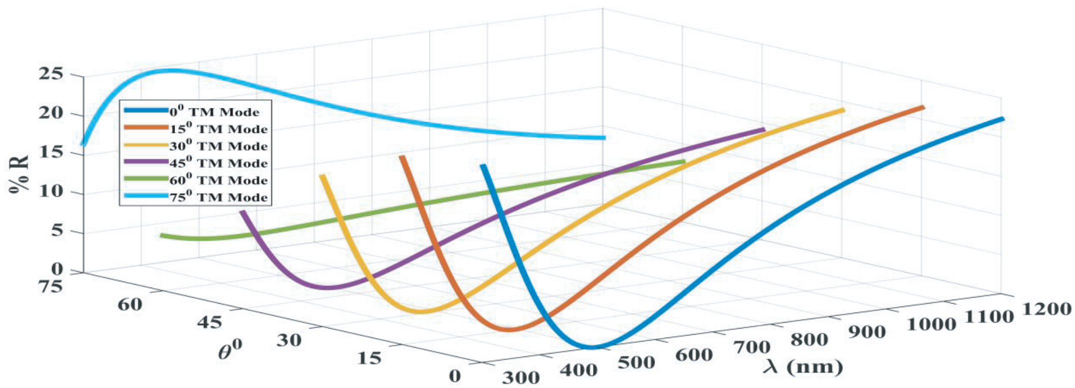

(a)

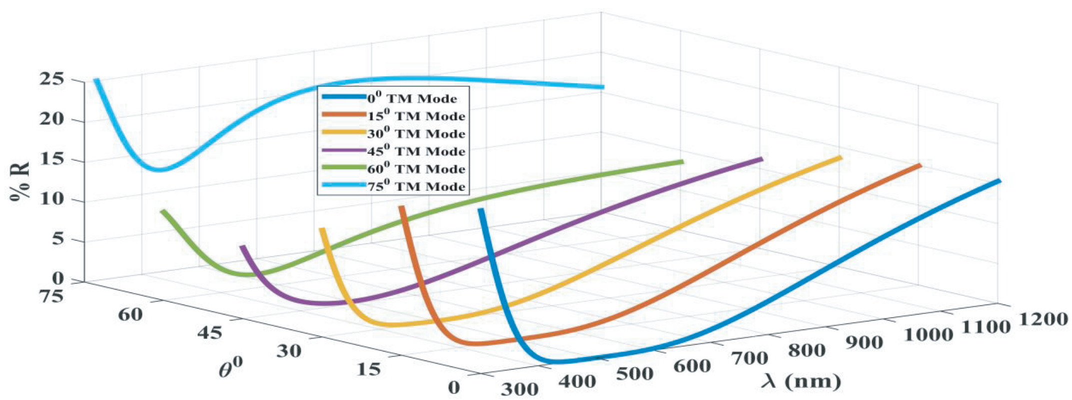

(b)

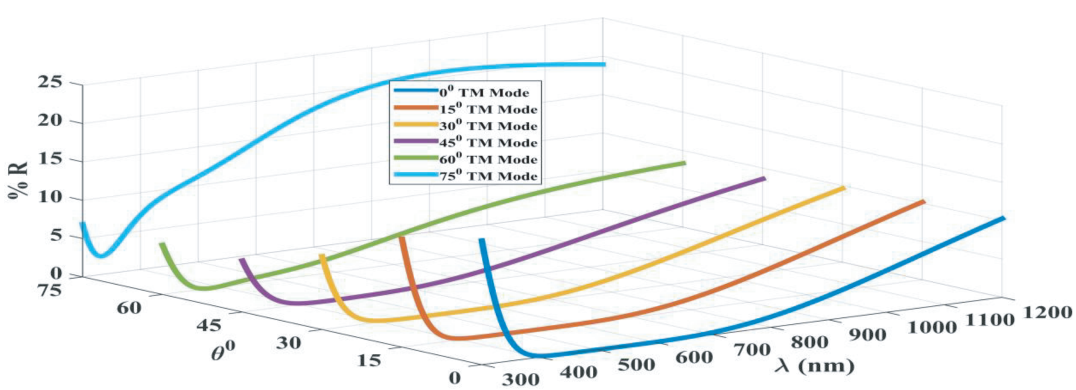

(c)

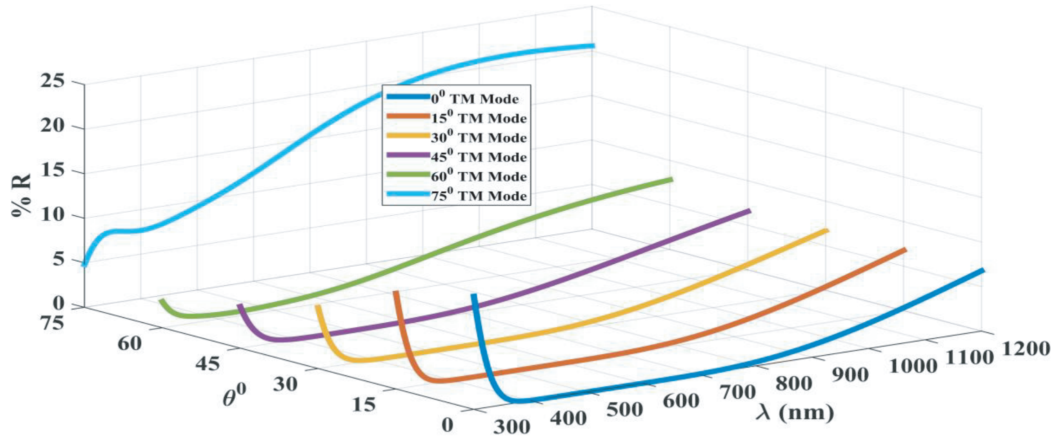

(d)

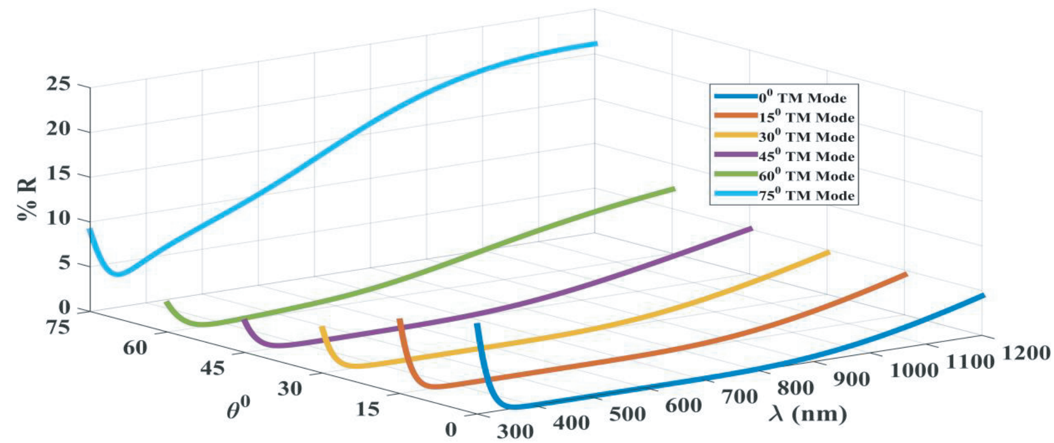

(e)

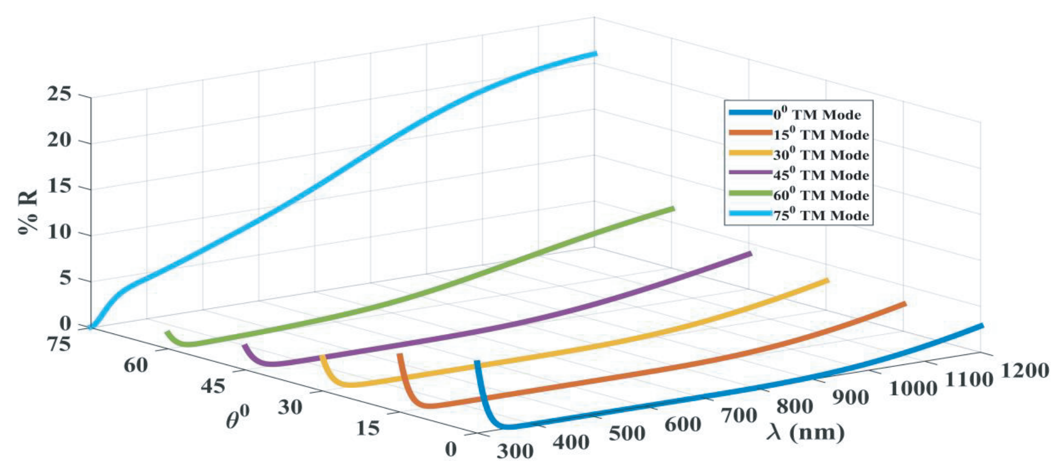

(f)

Figure 3. (a) Refection spectra of single coated materials in oblique incidence in TM mode. (b) Refection spectra of double coated materials in oblique incidence in TM mode. (c) Refection spectra of triple coated materials in oblique incidence in TM mode. (d) Refection spectra of four fold coated materials in oblique incidence in TM mode. (e) Refection spectra of five fold coated materials in oblique incidence in TM mode. (f) Refection spectra of six fold coated materials in oblique incidence in TM mode.

Table 3. Bandwidth for reflectance < 1% in oblique incidence for number of coated layers in TM mode.

Number of Coated layer	Band width $\Delta\lambda$ (nm) for reflectance < 1% in TM mode at angle of incidence					
	0°	15°	30°	45°	60°	75°
1	456.6 ~ 552.4 = 95.8	451.4 ~ 548.7 = 97.3	439 ~ 534.9 = 95.9	-	-	-
2	399.5 ~ 668.1 = 268.6	395.2 ~ 660.8 = 265	388.5 ~ 638.7 = 250.2	408.7 ~ 587 = 178.3	-	-
3	369.4 ~ 772.4 = 403	365.7 ~ 766.6 = 400.9	360 ~ 745.2 = 385.2	359.2 ~ 689.9 = 330.7	342.6 ~ 510.4 = 167.8	-
4	351.3 ~ 867.9 = 516.6	347.7 ~ 860.4 = 512.7	341.9 ~ 836.6 = 494.7	338.3 ~ 770.8 = 432.5	336.1 ~ 563.2 = 227.1	-
5	338.8 ~ 954.1 = 615.3	335.7 ~ 946.8 = 611.1	329.9 ~ 919.3 = 589.4	327.5 ~ 846.7 = 519.2	329.8 ~ 627.1 = 297.3	-
6	331.1 ~ 1033 = 701.9	326.9 ~ 1025 = 698.1	321.5 ~ 995.1 = 673.6	317.1 ~ 916.3 = 599.2	308.2 ~ 679.9 = 371.7	-

increases with the increase of N, and it decreases with the increase of angle θ. The calculated values are given in Table 3. Again in TM mode, the best result for nearly zero reflectance is obtained at $\theta = 0°$ and $N = 6$.

A comparison of Tables 2 and 3 indicates that TM mode shows better performance than in TE mode to get wider bandwidth for reflectance < 1% for all values of N.

Finally, we compare Fig. 4 with Fig. 1. Fig. 1 shows reflection spectra with theoretically calculated values of RI from Table 1. Unfortunately, natural occurring dielectrics of RI just equal to that obtained by calculations are not available. We have selected some materials for coating with nearly equal index values as shown in Table 4. Taking actual RI values, reflection spectra are drawn in Fig. 4. The details of reflectance, range, and bandwidth in spectral curves given in Fig. 1 and Fig. 4 are compared with each other as listed in Table 5. There is clear difference between Figs. 1 and 4, that the spectral curves show fluctuations in Fig. 4 compared to those in Fig. 1, and reflectance lies between 1% and 5% in practical dielectrics, although it confirms the validity of theory of ARC adopted in this work.

Table 4. List of dielectric materials with their refractive indices for ARC.

Number of Layers	Material used	Actual RI of used coated material
1	n_{11} = Silicon monoxide SiO	1.95
2	n_{21} = Bismuth oxide Bi_2O_3	2.45
	n_{22} = Magnesium fluoride MgF_2	1.38
3	n_{31} = As-S glass	2.77
	n_{32} = Silicon monoxide SiO	1.95
	n_{33} = Teflon	1.31
4	n_{41} = As-S glass	2.77
	n_{42} = Titanium dioxide TiO_2	2.40
	n_{43} = Lead fluoride PbF_2	1.73
	n_{44} = Teflon	1.31
5	n_{51} = As-S glass	2.77
	n_{52} = Titanium dioxide TiO_2	2.40
	n_{53} = Silicon monoxide SiO	1.95
	n_{54} = Lead fluoride PbF_2	1.73
	n_{55} = Teflon	1.31
6	Materials of such low R.I. values are unavailable	

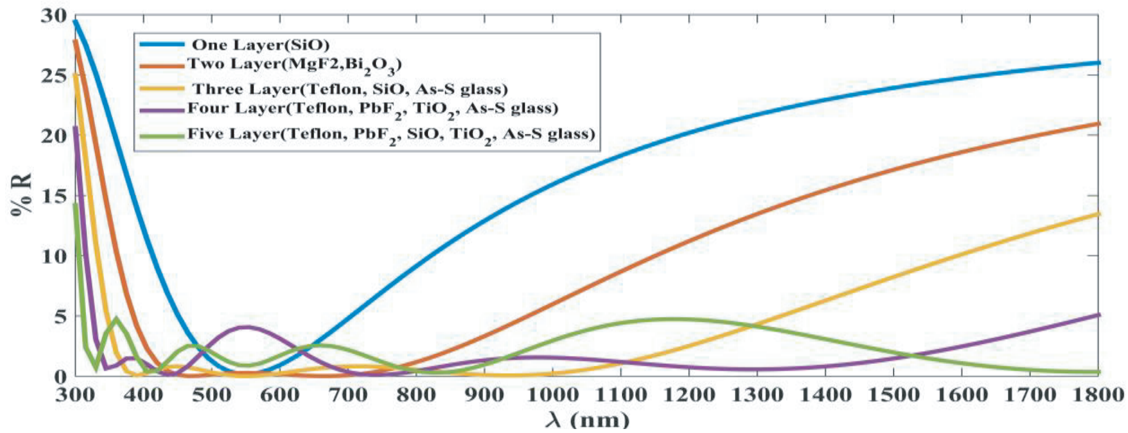

Figure 4. Reflection spectra for $N = 5$ with real available materials at $\theta = 0°$.

Table 5. Comparison between reflectance, range and bandwidth of reflection spectral curves according N given in Fig. 1 and Fig. 4.

No. of layers	From Fig. 1		From Fig. 4	
	Reflectance	Range and Bandwidth (nm)	Reflectance	Range and Bandwidth (nm)
$N = 1$	$< 1\%$	$457 \sim 552 = 95$	$< 1\%$	$506 \sim 602 = 96$
	$< 2\%$	$483 \sim 663 = 180$	$< 2\%$	$485 \sim 634 = 149$
	$< 3\%$	$470 \sim 663 = 193$	$< 3\%$	$472 \sim 659 = 187$
	$< 4\%$	$459 \sim 686 = 227$	$< 4\%$	$461 \sim 683 = 222$
	$< 5\%$	$450 \sim 707 = 257$	$< 5\%$	$451 \sim 704 = 253$
$N = 2$	$< 1\%$	$400 \sim 668 = 268$	$< 1\%$	$422 \sim 788 = 366$
	$< 2\%$	$422 \sim 788 = 366$	$< 2\%$	$409 \sim 845 = 436$
	$< 3\%$	$411 \sim 831 = 420$	$< 3\%$	$399 \sim 888 = 489$
	$< 4\%$	$402 \sim 871 = 469$	$< 4\%$	$392 \sim 925 = 532$
	$< 5\%$	$394 \sim 908 = 514$	$< 5\%$	$385 \sim 963 = 578$
$N = 3$	$< 1\%$	$370 \sim 773 = 403$	$< 1\%$	$369 \sim 1090 = 721$
	$< 2\%$	$394 \sim 915 = 521$	$< 2\%$	$360 \sim 1167 = 807$
	$< 3\%$	$384 \sim 873 = 489$	$< 3\%$	$356 \sim 1228 = 872$
	$< 4\%$	$376 - 1023 = 647$	$< 4\%$	$350 \sim 1283 = 933$
	$< 5\%$	$369 \sim 1073 = 704$	$< 5\%$	$347 \sim 1335 = 988$
$N = 4$	$< 1\%$	$352 \sim 868 = 516$	$< 1\%$	$340 \sim 361 = 21$, $405 \sim 469 = 64$, $666 \sim 859 = 193$
	$< 2\%$	$375 \sim 1023 = 648$	$< 2\%$	$337 \sim 485 = 148$, $633 \sim 1553 = 920$
	$< 3\%$	$367 \sim 1097 = 730$	$< 3\%$	$331 \sim 505 = 174$, $603 \sim 1645 = 1042$
	$< 4\%$	$361 \sim 1160 = 799$	$< 4\%$	$326 \sim 537 = 211$, $564 \sim 1722 = 1158$
	$< 5\%$	$355 \sim 1214 = 859$	$< 5\%$	$325 \sim 1794 = 1469$
$N = 5$	$< 1\%$	$339 \sim 954 = 615$	$< 1\%$	$319 \sim 331 = 12$, $395 \sim 431 = 36$, $532 \sim 568 = 36$, $759 \sim 901 = 142$
	$< 2\%$	$363 \sim 1140 = 777$	$< 2\%$	$316 \sim 336 = 20$, $386 \sim 448 = 62$, $500 \sim 610 = 110$, $710 \sim 952 = 242$
	$< 3\%$	$355 \sim 1213 = 858$	$< 3\%$	$315 \sim 341 = 26$, $380 \sim 1002 = 622$, $1408 \sim 2228 = 820$
	$< 4\%$	$350 \sim 1283 = 933$	$< 4\%$	$312 \sim 346 = 34$, $371 \sim 1063 = 652$, $1313 \sim 2322 = 1009$
	$< 5\%$	$346 \sim 1343 = 997$	$< 5\%$	$310 \sim 2407 = 297$

4. CONCLUSION

We have explained various aspects related to ARC in different ways with the help of spectral curves and also by tables prepared by calculations. We hope that our theoretical attempt to construct efficient high quality ARC will be valuable if it is done practically. We have shown the cases up to five layers of coatings and compared the curves with those of practical materials available. We could not show the practical case of six layer coating due to unavailability of materials of low RI approaching 1.0199. We hope that it will be possible in future by preparing synthetically artificial materials of very low index values approaching 1. Thus it would be an ideal ARC for PV cells to utilise incident light photons in maximum number taking up to six coatings to cover wide range of electromagnetic radiation. This is an attempt by which practically, all of humanity's energy requirements are satisfied by cheap, clean, and renewable sunlight.

REFERENCES

1. Cox, J. T. and G. Hass, *Antireflection Coatings Physics of Thin Films*, 239–304, ed. G. Hass and R. E. Thun, Academic, New York, 1964.
2. Knittl, Z., *Optics of Thin Films*, Wiley, London, 1976.
3. Yu, W., L. Shen, Y. Long, P. Shen, W. Guo, W. Chen, and S. Ruan, *Highly Efficient and High Transmittance Semitransparent Polymer Solar Cells with One-dimensional Photonic Crystals as Distributed Bragg Reflectors*, Published by Elsevier B.V., 2013.
4. Yu, W., X. Jia, Y. Long, L. Shen, Y. Liu, W. Guo, and S. Ruan, "Highly efficient semitransparent polymer solar cells with color rendering index approaching 100 using one-dimensional photonic crystal," *ACS Appl. Mater. Interfaces*, Vol. 7, 9920–9928, 2015.
5. Geetha Priyadarshini, B. and A. K. Sharma, "Design of multi-layer anti-reflection coating for terrestrial solar panel glass," *Bulletin of Materials Science*, Vol. 39, No. 3, 683–689, Indian Academy of Sciences, 2016.
6. Matsuoka, Y., S. Mathonnèire, S. Peters, and W. Ted Masselink, "Broadband multilayer anti-reflection coating for mid-infrared range from 7 μm to 12 μm," *Applied Optics*, Vol. 57, No. 7, 1645–1649, 2018.
7. Ismail Fathima, M. and K. S. Joseph Wilson, "Role of multilayer antireflective coating in ZnO based dye sensitized solar cell," Elsevier Ltd, 2019.
8. Deka, S. and W. Mohammed, "Enhancement of light absorption using nanoparticles embedded double layer anti reflection coating," *Engineering Journal*, 2020.
9. Guo, X., X. Quan, Z. Li, Q. Li, B. Zhang, X. Zhang, and C. Song, "Broadband anti-reflection coatings fabricated by precise time-controlled and oblique-angle deposition methods," *Coatings*, Vol. 11, 492, 2021.
10. Macleod, H. A., *Thin-Film Optical Filters*, Taylor & Francis, Milton Park, UK, 2010.
11. Walheim, S., E. Schäffer, J. Mlynek, and U. Steiner, *Nanophase-separated polymer films as high-performance antireflection coatings*, *Science*, Vol. 283, 520–522, 1999.
12. Deng, C. and H. Ki, "Pulsed laser deposition of refractive-index-graded broadband antireflection coatings for silicon solar cells," *Sol. Energy Mater. Sol. Cells*, Vol. 147, 37–45, 2016.
13. Uzum, A., M. Kuriyama, H. Kanda, Y. Kimura, K. Tanimoto, and S. Ito, "Non-vacuum processed polymer composite antireflection coating films for silicon solar cells," *Energies*, Vol. 9, 633, 2016.
14. Makableh, Y. F., R. Vasan, J. C. Sarker, A. I. Nusir, S. Seal, and M. O. Manasreh, "Enhancement of GaAs solar cell performance by using a ZnO sol-gel anti-reflection coating," *Sol. Energy Mater. Sol. Cells*, Vol. 123, 178–182, 2014.
15. Kosten, E. D., J. H. Atwater, J. Parsons, A. Polman, and H. Atwater, "Highly efficient GaAs solar cells by limiting light emission angle," *Light Sci. Appl.*, Vol. 2, e45, 2013.
16. Jung, S. M., Y. H. Kim, S. I. Kim, and S. I. Yoo, *Current Applied Physics*, Vol. 11, 538, 2011.
17. Schallenberg, U., "Design principles for broadband AR coatings," *Advances in Optical Thin Films III, Proc. of SPIE*, Vol. 7101, 710103-1, SPIE, 2008.
18. Vidal, B. and A. Fomier, "Nonquarterwave multilayer filters: Optical monitoring with a minicomputer allowing correction of thickness errors," *Appl. Opt.*, Vol. 18, 3857–3862, 1979.
19. Macleod, H. A., *Thin Film Optical Filters*, Institute of Physics, London, 2001.